Critical exponents at the three-loop level from stochastic continuum regularization

J. A. Alonso
Departamento de Matemática Aplicada, Escuela Técnica Superior de Ingenieros Industriales, José Gutierrez Abascal 2, 28006 Madrid, Spain

A. González Arroyo and C. P. Martín
Departamento de Física Teórica, C-XI, Universidad Autónoma de Madrid, Cantoblanco, 28049 Madrid, Spain

(Received 8 December 1987)

We compute the next-to-leading contributions to critical exponents using a recent method based on stochastic continuum regularization. Our best estimates are $\gamma = 1.2313$ and $\eta = 0.035$.

I. INTRODUCTION

The behavior of thermodynamical quantities at second-order phase transitions is determined by the critical exponents.[1] The theoretical computation of these experimental quantities is a test of our understanding of critical phenomena. By now, a wide variety of different techniques have been employed in attacking this program with considerable success. Some methods consist of the study of different models formulated on different lattices by resummation of the high-temperature series or Monte Carlo renormalization-group calculations.[2] These results give evidence in favor of universality. Another class of methods uses the framework of renormalized Euclidean quantum field theory. In this case the critical exponents are related to the anomalous dimensions of certain operators computed at the infrared stable zero of the β function of the corresponding field theory.[3] The position of this zero is of order $\epsilon = 4 - \omega$ and one can employ perturbative techniques in the vicinity of four dimensions.[4] One is, however, interested in computing at $\epsilon = 1$ and therefore resummation techniques are needed when computing to sufficiently high orders.[5] Another possibility[6] is to work directly in three dimensions and employ resummation methods to long perturbative series.[5]

Recently, new methods have been proposed[7,8] to compute the critical exponents in the context of renormalized quantum field theory. These new techniques are based on stochastic quantization.[9] This formulation of quantum field theory has led to new regularizations of the theory. One of them was introduced by Breit, Gupta, and Zaks[10] and modified by Alfaro[11] to remove a dimensioned cutoff in favor of a dimensionless parameter. A similar modification was introduced by us[8] to the regularization of Bern, Halpern, and Sadun.[12] The methods of Refs. 7 and 8 are essentially identical, differing only in the fact that they are based on the regularizations of Refs. 10 and Ref. 11, respectively. The main purpose of this paper is to extend the results of Ref. 8 to next-to-leading order. These results are given in the next three sections, where the method is reviewed for completeness. For a more detailed account the reader is referred to Ref. 8. Finally, the results and conclusions are collected in the last section. Comparison with other methods and comments upon further progress are also included. The main intermediate computations are presented in the Appendix.

II. LANGEVIN EQUATION WITH NONLOCAL NOISE TERM

In a previous paper,[8] following Ref. 12, we gave a modified version of Langevin equation which allows the regularization of stochastic correlation functions for a scalar field through a dimensionless parameter. This new Langevin equation is

$$\frac{\partial \Phi_0(x,t)}{\partial t} = -T_0 \frac{\delta S}{\delta \Phi_0(x,t)} + (-\Delta)^{-\sigma/2} \xi_0(x,t) . \tag{2.1}$$

$\Phi_0(x,t)$ being the stochastic scalar field in ω dimensions, S the classical-action functional for this field, and $\xi_0(x,t)$ the bare Gaussian stochastic noise

$$\langle \xi_0(x,t) \rangle = 0 ,$$
$$\langle \xi_0(x,t)\xi_0(x',t') \rangle = 2T_0 \delta(t-t')\delta^{(\omega)}(x-x') ,$$

where Δ stands for the Laplacian and σ is a dimensionless parameter.

The perturbative solution of Eq. (2.1) yields Φ_0 as a functional of the stochastic noise.[9] Then, we define the perturbative regularized Green functions as

$$G_{\text{reg}}(x_1, \ldots, x_n) = \lim_{t \to \infty} \langle \Phi_0(x_1 t), \ldots, \Phi_0(x_n, t) \rangle . \tag{2.2}$$

The value for the stochastic correlation functions can be obtained from the usual nonregularized stochastic diagrams[9] by substituting the ordinary crossed propagator by the following one:

$$\frac{e^{-K^2|t-t'|T}}{(K^2)^{\sigma+1}} , \tag{2.3}$$

where everything else is unchanged. t and t' are the stochastic times at the ends of the crossed line and K is the momentum flowing through it.

Let us choose an arbitrary stochastic diagram. As in any loop of this diagram there is, at least, one crossed propagator, it is obvious that the uv behavior of the loop can be improved by choosing a large enough positive σ. More precisely, considering (2.1) with the classical action S

$$S=\int d^{\omega}x\left[\tfrac{1}{2}\partial_{\mu}\Phi_0(x,t)\partial_{\mu}\Phi_0(x,t)+\frac{\lambda}{4!}\Phi_0^4(x,t)\right] \tag{2.4}$$

as our starting point, one may verify (Ref. 8) that the overall degree of divergence D of a stochastic diagram with E_o outgoing or crossed legs and E_i incoming lines is given by

$$D=(\omega-4-2\sigma)L+6+2\sigma-(3+2\sigma)E_i-E_o\ , \tag{2.5}$$

where L is the number of loops. Therefore, relying only on power counting, the diagram is rendered ultraviolet finite for some $\sigma>0$.

From now on we will work with both the σ complex and the ω complex and will assume that there is some domain in these two variables where all the integrals are well defined. These assumptions have been checked up to the order worked out in this paper. Furthermore, at $\sigma=\sigma^*=(\omega-4)/2=-\epsilon/2$ the theory is strictly renormalizable by power counting. In fact, from (2.5), the number of types of diagrams with $D\geq 0$ is finite. For $E_i=E_o=1$ we get $D=2$; for $E_i=2$, $E_o=0$, $D=+\epsilon$; and for $E_i=1$, $E_o=3$, $D=0$.

In order to regularize the theory we introduce a new parameter,

$$\rho=2(\sigma-\sigma^*)\ , \tag{2.6}$$

so that the uv infinities of the above-mentioned theories manifest themselves as poles in ρ. These infinities can be reabsorbed by renormalization of the parameters in the generalized Langevin equation (2.1), and, to do so, a MS prescription (subtraction of the pole part from divergent integrals) has been used.

Again, as in the previous case, there is no general proof of these statements though they have been checked at the three-loop level. Anyway, for a somewhat more general discussion of the subject, the reader is referred to Ref. 8.

We conclude the section with the renormalized Langevin equation

$$Z_t\frac{\partial\Phi_R}{\partial t}+T_RZ(-\Delta\Phi_R) =-\frac{\lambda_R}{3!}\mu^{2\sigma+\epsilon}T_RZ_v\Phi_R^3+Z_1(-\Delta)^{-\sigma/2}\xi_R\ , \tag{2.7}$$

$$\langle\xi_R(x,t)\xi_R(x',t')\rangle=2T_R\delta^{(\omega)}(x-x')\delta(t-t')\ , \tag{2.8}$$

$$\begin{aligned}&\Phi_R=Z_\Phi^{-1/2}\Phi_0,\quad Z_\Phi=Z_tZZ_1^{-2}\ ,\\&\xi_R=Z_\xi^{-1/2}\xi_0,\quad Z_\xi=ZZ_t^{-1}\ ,\\&T_0=T_RZ_\xi\ ,\\&\lambda_0=\lambda_R(\mu)\mu^\rho Z_\lambda,\quad Z_\lambda=Z_vZ^{-2}Z_t^{-1}Z_1^2\ ,\end{aligned} \tag{2.9}$$

where the scale μ has been introduced to render $\lambda_R(\mu)$ dimensionless.

III. THE β FUNCTION AND THE ANOMALOUS DIMENSIONS

This section is devoted to the computation of the β function and the anomalous dimensions of the field Φ and the operator Φ^2. Let us start with the function defined as

$$\beta(\lambda_R,\rho)=\mu\frac{d\lambda_R}{d\mu}\ . \tag{3.1}$$

Following the standard procedure, it is obtained from the identity

$$\lambda_0=\lambda_R\mu^\rho Z_\lambda\ , \tag{3.2}$$

where Z_λ has been computed to order λ_R^3,

$$Z_\lambda=1+\frac{\tilde{C}_1}{\rho}+\frac{\tilde{C}_2}{\rho^2}+O(\rho^{-3})\ , \tag{3.3}$$

with

$$\begin{aligned}&\tilde{C}_1=\lambda_R\left[3R+\frac{\lambda_R^2}{2}(-2\Omega+2R_\Phi+R_t)\right]\ ,\\&\tilde{C}_2=3!\tfrac{3}{2}R^2\lambda_R^2\ ,\end{aligned} \tag{3.4}$$

and Ω, R_Φ, R_t, and R are given by

$$\Omega=3!R^2\left[\frac{F(1,2-\epsilon/2;3-\epsilon/2;-1/3)}{3(4-\epsilon)}+\frac{F(1,1-\epsilon/2;2-\epsilon/2;-1/3)}{4}+\tfrac{1}{16}(1-\epsilon/2)J_{13}\right]\ , \tag{3.5}$$

$$R=\frac{(4\pi)^{\epsilon/2-2}}{\Gamma(2-\epsilon/2)}\ , \tag{3.6}$$

$$R_t=\frac{(4\pi)^{\epsilon-4}}{\Gamma^2(1-\epsilon/2)}\frac{F(1,1;2-\epsilon/2;1/4)}{(2-\epsilon)^2}\ , \tag{3.7}$$

$$R_\Phi=\frac{1}{2}\frac{(4\pi)^{\epsilon-4}}{\Gamma^2(1-\epsilon/2)(4-\epsilon)(2-\epsilon)^2}\times[(12-\epsilon)(2-\epsilon)F(1,1;2-\epsilon/2;1/4)-2F(2,1;2-\epsilon/2;1/4)]\ , \tag{3.8}$$

$$J_{13}=4\int_0^1dx\int_0^1dy\,x^{1-\epsilon/2}y^{-\epsilon/2}[(1-x)(3+x)-4x^2y(y-1)]^{-1}\ , \tag{3.9}$$

and F is the hypergeometric Gauss function (for more details see the Appendix).

Substituting (3.3) in (3.2), one gets the β function to order λ_R^3,

$$\beta(\lambda_R,\rho)=-\rho\lambda_R+\beta(\lambda_R)\ , \tag{3.10}$$

$$\beta(\lambda_R)=3R\lambda_R^2+\lambda_R^3(-2\Omega+2R_\Phi+R_t)\ . \tag{3.11}$$

Note that, as it should be, $\beta(\lambda_R,\rho)$ is finite when $\rho\to 0$. In fact it can easily be seen that up to λ_R^3 order,

$$\frac{\partial\tilde{C}_2}{\partial\lambda_R}-\tilde{C}_1\frac{\partial\tilde{C}_1}{\partial\lambda_R}-\lambda_R\left[\frac{\partial\tilde{C}_1}{\partial\lambda_R}\right]^2=0\ ,$$

which means that the double pole contribution vanishes. Note as well that from Eq. (3.10) one gets a fixed point λ_R^* of order ρ:

$$\lambda_R^*=\frac{\rho}{3R}+\rho^2\left[\frac{2\Omega-2R_\Phi-R_t}{27R^3}\right]+O(\rho^3) \tag{3.12}$$

and this assures the validity of perturbation theory for $\lambda_R=\lambda_R^*$ and $\rho\sim 0$.

Let us go now to the subject of the anomalous dimension $\gamma_\Phi(\lambda_R,\rho)$, defined as

$$\gamma_\Phi(\lambda_R,\rho)=\mu\frac{\partial}{\partial\mu}\ln Z_\Phi\ , \tag{3.13}$$

where, according to (2.9),

$$Z_\Phi=ZZ_tZ_1^{-2} \tag{3.14}$$

and

$$\begin{aligned}&Z=1+\frac{a_1}{\rho}+\frac{a_2}{\rho^2}+\cdots\ ,\\&Z_t=1+b_1/\rho+b_2/\rho^2+\cdots\ ,\\&Z_1=1\ ,\end{aligned} \tag{3.15}$$

with a_1,a_2, and b_1,b_2 computed up to the three-loop level. As a_2 and b_2 do not contribute to the $\gamma_\Phi(\lambda_R,\rho)$ function, only the expressions for a_1 and b_1 are given as

$$a_1=a_1^{(2)}\lambda_R^2+a_1^{(3)}\lambda_R^3,\quad b_1=b_1^{(2)}\lambda_R^2+b_1^{(3)}\lambda_R^3\ , \tag{3.16}$$

where $a_1^{(2)}$, $a_1^{(3)}$, $b_1^{(2)}$, and $b_1^{(3)}$ are collected in the Appendix.

From (3.13) and (3.16) one gets

$$\gamma_\Phi(\lambda_R,\rho)=-2\lambda_R^2(a_1^{(2)}+b_1^{(2)})-3\lambda_R^3(b_1^{(3)}+a_1^{(3)}) \tag{3.17}$$

and taking into account (3.12)

$$\gamma_\Phi(\lambda_R^*)=\rho^2\frac{R_t+R_\Phi}{9R^2}+\frac{\rho^3}{27R^3}\left[\frac{2(2\Omega-R_\Phi-R_t)(R_t+R_\Phi)}{3R}-3(a_1^{(3)}+b_1^{(3)})\right]. \tag{3.18}$$

Finally we will be concerned with the computation of the anomalous dimension γ_{Φ^2}. For that purpose we add to the classical action S appearing in Eq. (2.1) a mass operator piece $\frac{1}{2}M_0\Phi_0^2(x,t)$. After renormalization we get

$$\begin{aligned}Z_t\frac{\partial\Phi_R}{\partial t}+T_RZ(-\Delta\Phi_R)=&-\lambda_R\frac{\mu^{2\sigma+\epsilon}}{3!}T_RZ_v\Phi_R^3\\&-T_RZ_MM_R\Phi_R(x,t)\\&+(-\Delta)^{-\sigma/2}\xi_R(x,t)\ ,\end{aligned} \tag{3.19}$$

where

$$M_0=Z_{\Phi^2}M_R,\quad Z_{\Phi^2}=Z_MZ_t^{1/2}Z^{-3/2}\ . \tag{3.20}$$

The computation of Z_M to order λ_R^2 yields (see the Appendix for details)

$$\begin{aligned}&Z_M=1+\frac{\lambda_RR}{\rho}+\lambda_R^2\left[2\frac{R^2}{\rho^2}-\frac{R^2a_M}{\rho}\right],\\&a_M=\frac{1}{3}\frac{F(1,2-\epsilon/2;3-\epsilon/2,-1/3)}{4-\epsilon}\\&\qquad+\tfrac{1}{2}F(1,1-\epsilon/2;2-\epsilon/2;-1/3)\ ,\end{aligned} \tag{3.21}$$

and from (3.20) and (3.21) and the definition of γ_{Φ^2},

$$\gamma_{\Phi^2}=\mu\frac{\partial}{\partial\mu}\ln Z_{\Phi^2}\ , \tag{3.22}$$

one finally gets

$$\gamma_{\Phi^2}(\lambda_R)=-\lambda_RR+\lambda_R^2\left[2R^2a_M+\frac{R_t}{2}-\frac{3}{2}R_\Phi\right] \tag{3.23}$$

and once again the double pole contribution vanishes. At the fixed point $\lambda_R=\lambda_R^*$

$$\gamma_{\Phi^2}(\lambda_R^*)=-\rho/3+\frac{\rho^2}{9R^2}\left[2R^2a_M-\frac{2\Omega-2R_\Phi-R_t}{3}+\frac{R_t}{2}-\frac{3}{2}R_\Phi\right]. \tag{3.24}$$

IV. CRITICAL EXPONENTS

Our aim is to apply the results of previous section to the computation of critical exponents in three dimensions. They will be obtained from renormalized quantum field theory, in an analogous way to Ref. 4.

To begin with, let us define the critical exponents η,γ for general ρ,ϵ:

$$\begin{aligned}&\eta(\rho,\epsilon)=\gamma_\Phi(\lambda_R^*)\ ,\\&\gamma(\rho,\epsilon)=\left[1+\frac{\gamma_{\Phi^2}(\lambda_R^*)}{2-\eta(\rho,\epsilon)}\right]^{-1},\end{aligned} \tag{4.1}$$

where the physical point corresponds to $\rho=\epsilon=1$.

As we have just seen, perturbation theory allows the computation of $\eta(\rho,\epsilon)$ and $\gamma(\rho,\epsilon)$ in powers of ρ for arbitrary ϵ. Thus, defining a new variable $\epsilon=\epsilon^*+(1-\epsilon^*)\rho$, $\eta[\rho,\epsilon^*+(1-\epsilon^*)\rho]$, and $\gamma[\rho,\epsilon^*+\rho(1-\epsilon^*)]$ can be computed as power series of ρ and, after that, the physical limit $\rho=1$ should be taken.

In doing so, Eqs. (3.18), (3.24), and (4.1) lead, after a straightforward calculation, to

$$\eta_{\rm phys}(\epsilon^*)=\eta_2(\epsilon^*)+\eta_3(\epsilon^*)+(1-\epsilon^*)\frac{\partial\eta_2(\epsilon^*)}{\partial\epsilon^*}\ , \tag{4.2}$$

where

$$\eta_2(\epsilon^*)=\frac{R_t+R_\Phi}{9R^2}\ ,$$
$$\eta_3(\epsilon^*)=\frac{1}{27R^3}\left[\frac{2(2\Omega-2R_\Phi-R_t)(R_t+R_\Phi)}{3R}-3(a_1^{(3)}+b_1^{(3)})\right]\ , \tag{4.3}$$
$$\gamma_{\rm phys}(\epsilon^*)=1+\frac{1}{6}+\frac{1}{2}\left[\frac{1}{18}-\frac{1}{9R^2}\left[2R^2a_M-\frac{2\Omega-2R_\Phi-R_t}{3}+\frac{1}{2}R_t-\frac{3}{2}R_\Phi\right]\right]\ ,$$

where Ω, R, R_t, R_Φ, $a_1^{(3)}$, $b_1^{(3)}$, and a_M have been defined in Eqs. (3.5)–(3.8), (3.16), and (3.21). It is worth noticing that the above obtained expressions are a family of physical critical exponents, parametrized by ϵ^*.

V. CONCLUSIONS

One of the characteristic properties of our method is that the whole procedure depends on an arbitrary parameter ϵ^*. It is natural to expect the best determination of the critical exponents to lie in the vicinity of $\epsilon^*=1$, since in that case we lie closer to physical point $\epsilon=1$. Our results are shown in Table I and Fig. 1 for ϵ^* varying between 0 and 1.5 (at $\epsilon^*=2$ our formulas become singular).

Let us first consider the critical exponent γ. The lowest-order result is $\gamma=\frac{5}{6}$ (independent of ϵ^*). The next-to-leading correction term is always positive and varies slightly with ϵ^* in the region of interest. The best estimate can be selected by choosing the value of ϵ^* where the correction is smallest. The result is $\gamma=1.2313$ obtained at $\epsilon^*=0.9$. Notice, however that in the whole region plotted, γ only differs by 0.013.

For η the situation is very different. The next-to-leading correction is, in general, very large. This correction is 10% or less of the leading-order term in a region ranging from $\epsilon^*=1.125$ to 1.16. Within this region the correction changes sign from positive to negative. Our best estimate $\eta=0.035$ comes from $\epsilon^*=1.143$ where the correction vanishes. Within the 10% correction region η varies by ±0.005.

Let us now compare our results with those of other methods. The best results obtained up to now by different techniques are $\gamma=1.239(3)$ and $\eta=0.031(4)$.[2,5] The results obtained with the ϵ expansion to next-to-leading order are[4] $\gamma=1.244$ and $\eta=0.037$. Relative to the latter technique our estimates seem to be worse for γ, but better for η and even consistent with the best determinations. The results obtained by series expansion only become of better accuracy once care is taken with the subleading confluent singularities predicted by the renormalization group.[2] For comparison, we also show in Fig. 1 the result of Ref. 13. The error bar shown is due to numerical errors in the evaluation of the integrals of that method. One nice advantage of our method compared to theirs (Refs. 7 and 13) is that the computations are substantially simplified.

We want to conclude this section with a few considerations for possible future improvement. All the calcula-

TABLE I. $\eta_{\rm phys}$ and $\gamma_{\rm phys}$ for some values of ϵ^*.

ϵ^*	η_3	$\eta_2^1=\frac{\partial\eta_2}{\partial\epsilon^*}(1-\epsilon^*)$	η_2	$\eta_{\rm phys}=\eta_2+\eta_2^1+\eta_3$	$\gamma_{\rm phys}$
0.0	5.369×10^{-2}	6.568×10^{-2}	9.080×10^{-2}	0.2101	1.2372
0.3	5.087×10^{-2}	5.068×10^{-2}	7.902×10^{-2}	0.1805	1.2347
0.5	4.496×10^{-2}	3.991×10^{-2}	7.032×10^{-2}	0.1551	1.2331
0.7	4.227×10^{-2}	2.733×10^{-2}	6.078×10^{-2}	0.1303	1.2319
0.8	3.880×10^{-2}	1.980×10^{-2}	5.560×10^{-2}	0.1142	1.2315
0.9	3.450×10^{-2}	1.080×10^{-2}	5.022×10^{-2}	9.568×10^{-2}	1.2313
1.0	2.940×10^{-2}	0	4.449×10^{-2}	7.394×10^{-2}	1.2314
1.1	2.300×10^{-2}	-1.370×10^{-2}	3.840×10^{-2}	4.771×10^{-2}	1.2318
1.2	1.480×10^{-2}	-3.180×10^{-2}	3.192×10^{-2}	1.491×10^{-2}	1.2329
1.3	5.310×10^{-3}	-5.660×10^{-2}	2.498×10^{-2}	-2.629×10^{-2}	1.2343
1.4	-6.92×10^{-3}	-9.190×10^{-2}	1.753×10^{-2}	-8.127×10^{-2}	1.2391
1.5	-2.38×10^{-2}	-0.144	9.504×10^{-3}	-0.1592	1.2444

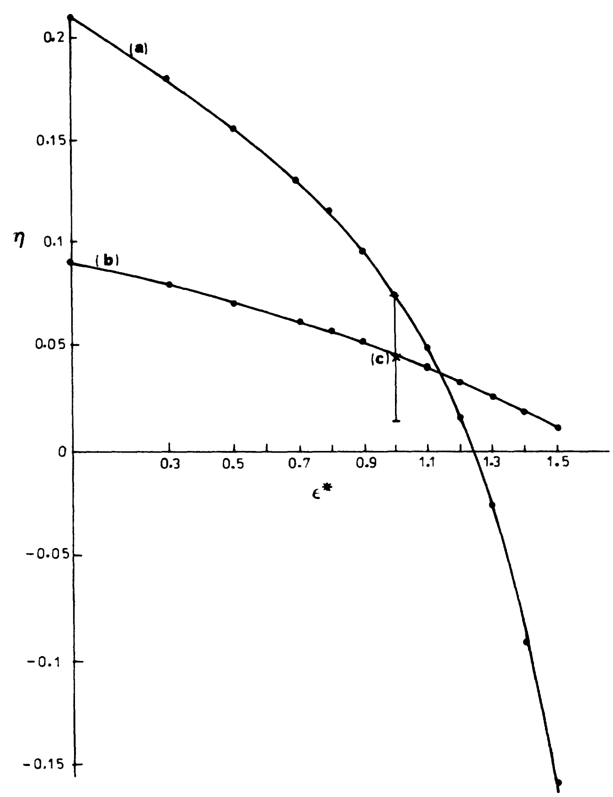

FIG. 1. The critical exponent $\eta_{\rm phys}$ as a function of ϵ^*. The curves (a) and (b) are, respectively, the contributions at the three- and two-loop levels. (c) is the value given in Ref. 13.

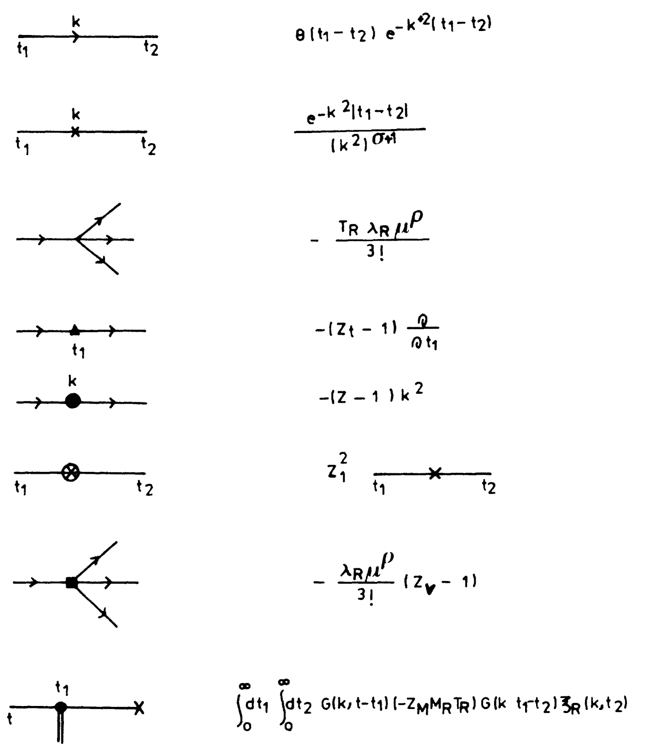

FIG. 2. Diagrammatic rules from Eq. (3.19).

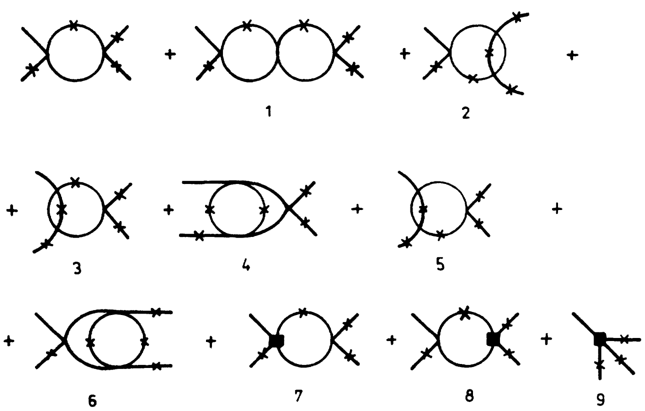

FIG. 3. Diagrams contributing to Z_v.

tions done by now have been done by hand. If one wishes to go to higher-loop orders one should rather employ computers. Can one improve the result by computing to one more loop order? In the case of the ϵ expansion the results to that order start departing from the best estimates[14] according to the asymptotic character of the expansion. This may or may not be the case for the ρ expansion presented in this paper. Notice, for example, that our results for γ approach the best estimate from below, while for the ϵ-expansion case they oscillate around it.

If higher orders are computed, resummation methods will presumably be helpful. However, notice[5] that one does not substantially improve with respect to the next-to-leading result in the case of the ϵ expansion. Nevertheless, resummation methods are helpful in providing errors bars to the truncated approximations.

In conclusion, we think that our result exemplifies the usefulness of the Langevin equation regularization applied to a classical problem as that of the computation of critical exponents. The accuracy of our best estimates is very encouraging, and add to the large class of methods which have been employed in this task.

ACKNOWLEDGMENTS

This work has been partially supported by Comisión Asesora de Investigación Científica y Técnica (CAICyT).

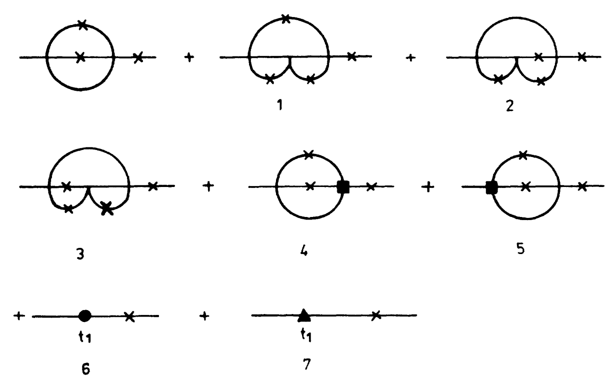

FIG. 4. Diagrams contributing to Z, Z_t.

APPENDIX

In this Appendix we show the main steps leading to the computation of the Z's that renormalize the Langevin equation to order λ_R^3.

By writing Eq. (2.7) as

$$\frac{\partial}{\partial t}\Phi_R(x,t)+T_R(-\Delta)\Phi_R(x,t)-(-\Delta)^{-\sigma/2}\xi_R(x,t)$$
$$=-(Z_t-1)\frac{\partial}{\partial t}\Phi_R(x,t)-T_R(Z-1)(-\Delta)\Phi_R(x,t)-\frac{T_R\lambda_R\mu^\rho}{3!}Z_v\Phi^3(x,t)+(Z_1-1)(-\Delta)^{-\sigma/2}\xi_R(x,t)\ , \quad \text{(A1)}$$

and following the standard iterative process one easily gets the stochastic diagrams and their counterterms. From these diagrams and using the rules of Fig. 2, the stochastic correlation functions can be obtained. The divergent diagrams contributing to the four- and two-point stochastic correlation functions, up to λ_R^2 and λ_R^3, respectively, are shown in Figs. 3 and 4. The counterterms are chosen in such a way that they cancel the pole part of the uv divergences.

Once the subdivergences have been subtracted from diagrams (1)–(6) by adding diagrams 7 and 8 (see Fig. 3), the only remaining divergence is a local one. The contributions from the different diagrams are listed below:

diagram 1:

$$-\lambda_R T_R\mu^\rho(3\lambda_R^2T_R^2\,\mathrm{inf}I_1)\ ,$$

diagram 2:

$$-\lambda_R T_R\mu^\rho(3!\lambda_R^2T_R^2\,\mathrm{inf}I_2)\ ,$$

diagram 3:

$$-\lambda_R T_R\mu^\rho(3\lambda_R^2T_R^2\,\mathrm{inf}I_3)\ ,$$

diagram 4:

$$-\lambda_R T_R\mu^\rho(3/2\lambda_R^2T_R^2\,\mathrm{inf}I_4)\ , \quad \text{(A2)}$$

diagram 5:

$$-\lambda_R T_R\mu^\rho(3\lambda_R^2T_R^2\,\mathrm{inf}I_5)\ ,$$

diagram 6:

$$-\lambda_R T_R\mu^\rho(3/2\lambda_R^2T_R^2\,\mathrm{inf}I_6)\ ,$$

where

$$\mathrm{inf}I_1=-\frac{R^2}{\rho^2},\quad \mathrm{inf}I_2=R^2\left[-\frac{1}{2\rho^2}+\frac{1}{\rho}\left[\frac{1}{6}\frac{F(1,2-\epsilon/2;3-\epsilon/2;-1/3)}{4-\epsilon}\right]\right]\ ,$$

$$\mathrm{inf}I_3=\mathrm{inf}I_2,\quad \mathrm{inf}I_4=\frac{1}{\rho}\frac{R^2}{3}F(1,1-\epsilon/2;2-\epsilon/2,-1/3)\ ,$$

$$\mathrm{inf}I_5=\mathrm{inf}I_2+\mathrm{inf}I_4,\quad \mathrm{inf}I_6=\frac{1}{\rho}\frac{R^2}{4}(1-\epsilon/2)J_{13}\ ,$$

$$R=\frac{(4\pi)^{\epsilon/2-2}}{\Gamma(2-\epsilon/2)}\ ,$$

$$J_{13}=4\int_0^1dx\int_0^1dy\,x^{1-\epsilon/2}y^{-\epsilon/2}[(1-x)(3+x)-4x^2y(y-1)]^{-1}\ .$$

Adding (A2) and the lower-order contribution, one gets the value of Z_v at the two-loop level

$$Z_v=1+\frac{C_1}{\rho}+\frac{C_2}{\rho^2}+\cdots\ , \quad \text{(A3)}$$

with

$$C_2=3!(\tfrac{3}{2}R^2\lambda_R^2),\quad C_1=3\lambda_R R-\lambda_R^2\Omega$$

and Ω given in (3.5).

The single pole contributions to Z coming from the diagrams in Fig. 4 are the following:

diagram 1:

$$-\lambda_R^3a^{(1)}\ , \quad \text{(A4)}$$

diagrams 2 and 3:

$$-\lambda_R^3(a^{(2)}+\hat{a}^{(2)})\ ,$$

where

$$a^{(1)}=-\frac{2}{(4\pi)^{6-3\epsilon/2}\Gamma^3(2-\epsilon/2)}\left[-\frac{J_2}{24}(1-\epsilon/2)+F(1,1-\epsilon/2;2-\epsilon/2;-1/3)\times\left[\frac{\gamma+\Psi(1-\epsilon/2)}{18}+\frac{F(1,2-\epsilon/2;3-\epsilon/2;-1/3)}{27(2-\epsilon/2)}\right]\right]$$

$$+\frac{1}{(4\pi)^{6-3\epsilon/2}\Gamma^2(2-\epsilon/2)\Gamma(3-\epsilon/2)}\left[\frac{1}{24}(1-\epsilon/2)J_3+\frac{8}{81}\frac{1}{2-\epsilon/2}F(1,2-\epsilon/2;3-\epsilon/2;-1/3)\times F(2,1-\epsilon/2,2-\epsilon/2;-1/3)\right.$$

$$-\frac{4}{81}\frac{1}{(2-\epsilon/2)^2}F(1,2-\epsilon/2;3-\epsilon/2;-1/3)F(2,1-\epsilon/2;3-\epsilon/2;-1/3)$$

$$+\frac{2}{27}\frac{1}{2-\epsilon/2}F(2,1-\epsilon/2;3-\epsilon/2;-1/3)[1-\gamma-\Psi(1-\epsilon/2)]$$

$$\left.+\frac{4}{27}\left[F(1,1-\epsilon/2;2-\epsilon/2;-1/3)-\frac{F(1,1-\epsilon/2;3-\epsilon/2;-1/3)}{4-\epsilon}\right]^2\right],$$

$$a^{(2)}=\frac{1}{6(4\pi)^{6-3\epsilon/2}\Gamma^2(1-\epsilon/2)\Gamma(2-\epsilon/2)}\left[\frac{J_4}{2}+J_5\left[\frac{2}{2-\epsilon}-\frac{2}{12-3\epsilon}F(1,2-\epsilon/2;3-\epsilon/2;-1/3)\right]\right.$$

$$-\frac{2}{4-\epsilon}J_6+\frac{8}{12-3\epsilon}J_7F(1,1-\epsilon/2;2-\epsilon/2,-1/3)$$

$$\left.-\frac{4}{6-3\epsilon}J_8\left[F(1,1-\epsilon/2;2-\epsilon/2;-1/3)-\frac{4}{12-3\epsilon}F(2,1-\epsilon/2;2-\epsilon/2;-1/3)\right]\right],$$

$$\hat{a}^{(2)}=\frac{-1}{6(4\pi)^{6-3\epsilon/2}\Gamma^3(1-\epsilon/2)}J_9\ ,$$

and

$$J_2=\int_0^1 dx\frac{4x^{-\epsilon/2}}{3+x}\ln\frac{4x}{(3+x)(1-x)},\quad J_3=\int_0^1 dx\frac{16x^{-\epsilon/2}(1-x)}{(3+x)^2}\ln\frac{4x}{(3+x)(1-x)}\ ,$$

$$J_4=\int_0^1 dy\int_0^1 dz\, a(y,z)b(y,z)\ln\frac{y^2z(1-z)}{\lambda^2(y,z)},\quad J_5=\int_0^1 dy\int_0^1 dz\, a(y,z)b(y,z)\ ,$$

$$J_6=\int_0^1 dy\int_0^1 dz\, a(y,z)\left[\frac{1-y}{2\lambda(y,z)}\right]^2,\quad J_7=\int_0^1 dy\int_0^1 dz\, a(y,z)\left[\frac{1-y}{2\lambda(y,z)}\right],$$

$$J_8=\int_0^1 dy\int_0^1 dz\, a(y,z)\ ,$$

$$a(y,z)=y^{(1-\epsilon)}\lambda^{\epsilon/2-1}(1-z)^{-\epsilon/2}z^{-\epsilon/2}\ ,$$

$$b(y,z)=\frac{1-y}{2\lambda}\left[1-\frac{1-y}{2\lambda}\right],$$

$$\lambda(y,z)=1-\frac{(1+y)^2}{4}+y^2z(1-z)\ ,$$

$$J_9=\int_0^1 dx\int_0^1 dy\, x^{1-\epsilon}y^{-\epsilon/2}(1-y)^{-\epsilon/2}(1-x)^{\epsilon/2-1}\int_0^1 dz\int_0^1 d\theta\left[z(z\theta)^{-\epsilon/2}(1-z)^{-\epsilon/2}m^{-2+\epsilon/2}\left[\frac{z(1-\theta)}{2}-\frac{z^2(1-\theta)^2}{4b}\right]\right],$$

$$m = z(1-\theta)+(1-z)n - \frac{(1-z\theta)^2}{4} ,$$

$$n = \frac{x^2 y(1-y)}{1-x} + \frac{3+x}{4} .$$

In an analogous way, for Z_t,

$$\begin{aligned} &\text{diagram 1:} \\ &\quad -\lambda_R^3 b^{(1)} , \\ &\text{diagrams 2 and 3:} \\ &\quad 0 , \end{aligned} \tag{A5}$$

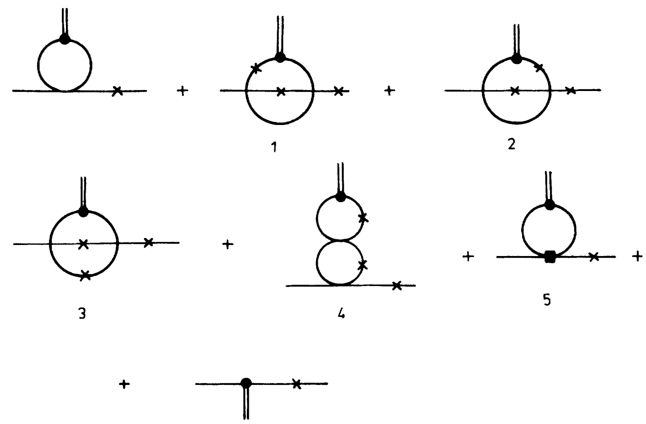

FIG. 5. Diagrams contributing to Z_M.

with

$$b^{(1)} = -\frac{2}{(4\pi)^{6-3\epsilon/2}\Gamma^3(2-\epsilon/2)} \left[-\frac{J_2}{24}(1-\epsilon/2)+F(1,1-\epsilon/2;2-\epsilon/2;-1/3) \times \left[\frac{F(1,2-\epsilon/2;3-\epsilon/2;-1/3)}{27(2-\epsilon/2)} + \frac{\gamma+\Psi(1-\epsilon/2)}{18} \right] \right] .$$

Taking into account the previous results and the lower-order contributions

$$Z = 1+\frac{a_1}{\rho}+O(\rho^{-2}) ,$$
$$Z_t = 1+\frac{b_1}{\rho}+O(\rho^{-2}) , \tag{A6}$$

where

$$a_1 = a_1^{(2)}\lambda_R^2 + a_1^{(3)}\lambda_R^3, \quad b_1 = \lambda_R^2 b_1^{(2)} + b_1^{(3)}\lambda_R^3 ,$$
$$a_1^{(2)} = -\frac{R_\Phi}{2}, \quad b_1^{(2)} = -\frac{R_t}{2} ,$$
$$a_1^{(3)} = -(a^{(1)}+a^{(2)}+\hat{a}^{(2)}), \quad b_1^{(3)} = -b^{(1)} .$$

According to (A3) and (A6), and after some algebra, one obtains (3.3). The contribution to the renormalization of Langevin equation of diagrams with $E_i = 2E_0 = 0$ is zero because they are finite when $\epsilon \neq 0$. Thus, $Z_1 = 1$.

Finally, we compute Z_M as defined in (3.19). The diagrams that contribute are shown in Fig. 5. Their contributions are

$$\begin{aligned} &\text{diagram 1:} \\ &\quad \lambda_R^2 \,\mathrm{inf} I_2 , \\ &\text{diagram 2:} \\ &\quad \lambda_R^2 \,\mathrm{inf} I_5 , \\ &\text{diagram 3:} \\ &\quad \tfrac{1}{2}\lambda_R^2 \,\mathrm{inf} I_4 , \\ &\text{diagram 4:} \\ &\quad \lambda_R^2 \,\mathrm{inf} I_1 , \end{aligned} \tag{A7}$$

where the meaning of $\mathrm{inf}I_1$, $\mathrm{inf}I_2$, $\mathrm{inf}I_4$, and $\mathrm{inf}I_5$ has been given before. From (A7) and the lower-order result quoted in Ref. 8, one easily obtains (3.21).

[1]For an early introduction to the subject see H. E. Stanley, *Introduction to Phase Transitions and Critical Phenomena* (Oxford University Press, London, 1971). For more recent experimental results see *Phase Transitions,* Proceedings of the 1980 Cargese Summer School, Cargese 1980, edited by M. Levy, J. C. Le Guillou, and J. Zinn-Justin (Plenum, New York, 1982).

[2]*Phase Transitions and Critical Phenomena,* edited by C. Domb and M. S. Green (Academic, New York, 1974), Vol. 3; J. Adler, J. Phys. A **16**, 3585 (1983), and references therein; G. S. Pawley *et al.*, Phys. Rev. B **29**, 4030 (1984).

[3]K. G. Wilson and J. B. Kogut, Phys. Rep. C **12**, 75 (1974); E. Brezin, J. C. Le Guillou, and J. Zinn-Justin, in *Phase Transitions and Critical Phenomena,* edited by C. Domb and M. S. Green (Academic, New York, 1976), Vol. 6; D. J. Amit, *Field Theory, the Renormalization Group and Critical Phenomena* (McGraw-Hill, New York, 1978).

[4]K. G. Wilson and M. E. Fisher, Phys. Rev. Lett. **28**, 240 (1972); K. G. Wilson, *ibid.* **28**, 548 (1972); E. Brezin, J. C. Le Guillou, and J. Zinn-Justin, Phys. Rev. D **8**, 434 (1973).

[5]J. C. Le Guillou and J. Zinn-Justin, Phys. Rev. B **21**, 3976 (1980), and references therein.

[6]G. Parisi, in *Proceedings of the 1973 Cargese Summer School,* edited by E. Brezin and J. M. Charap [J. Stat. Phys. **2**, 16 (1979)]; G. A. Baker *et al.*, Phys. Rev. Lett. **36**, 1351 (1976).

[7]J. Alfaro, R. Jengo, and N. Parga, Phys. Rev. Lett. **54**, 369 (1985).

[8]A. González-Arroyo and C. P. Martin (unpublished).
[9]G. Parisi and Y. Wu, Sci. Sin. **24**, 483 (1981); H. Hüffel and P. Damgaard, Phys. Rep. (to be published); A. A. Migdal, Usp. Fiz. Nauk **149**, 3 (1986) [Sov. Phys.—Usp. **29**, 389 (1986)].
[10]J. D. Breit, S. Gupta, and Z. Zaks, Nucl. Phys. **B233**, 61 (1982).
[11]J. Alfaro, Nucl. Phys. **B253**, 464 (1985).
[12]Z. Bern, M. B. Halpern, L. Sadun, and C. Taubes, Nucl. Phys. **B2841** (1987); **B284**, 35 (1987); Z. Bern, M. B. Halpern and L. Sadun, *ibid.* **B284**, 92 (1987); Z. Phys. C **35**, 255 (1987); Z. Bern, M. B. Halpern, and N. G. Kalivas, Phys. Rev. D **35**, 753 (1987); Z. Bern, M. B. Halpern, and H. S. Chau, Z. Phys. C **34**, 267 (1987); M. B. Halpern, Phys. Lett. (to be published).
[13]R. Jengo and S. Pugnetti (unpublished).
[14]E. Brezin, J. C. Le Guillou, J. Zinn-Justin, and B. G. Nickel, Phys. Lett. **44A**, 227 (1973).